Two-photon diagnostics of stress-induced exciton traps and loading of 1*s*-yellow excitons in Cu_2O

N. Naka and N. Nagasawa
Department of Physics, Graduate School of Science, University of Tokyo, 7-3-1 Hongo, Bunkyo-ku, Tokyo 113-0033, Japan
(Received 29 June 2001; published 31 January 2002)

Two-photon spectroscopy is applied to stress-induced exciton traps for 1*s* yellow excitons in Cu_2O crystals at 1.6 K. The resonance emission lines associated with orthoexcitons and paraexcitons are used to measure the shape and depth of the traps for respective species of excitons. The luminescence from paraexcitons shows well-resolved structure suggesting their drift motion toward the bottom of the trap. The transit time of the drift is evaluated to be 0.2 μs from the peak energy of the structure. This value is comparable to the decay time of paraexciton luminescence of 0.3 μs under 2.4 kbar stress measured by time-resolved spectroscopy. The decay time under the stress is slightly shorter than that with zero stress (0.6 μs), but is enough to establish the cooling of the paraexciton system.

DOI: 10.1103/PhysRevB.65.075209 PACS number(s): 71.35.−y; 78.55.−m

I. INTRODUCTION

Since Bose-Einstein condensation (BEC) of excitonic systems in semiconductors has been proposed, many experimental efforts have been devoted to the realization. One attractive approach is that to make a stress-induced exciton trap in order to capture the excitons, preventing the density decrease due to the diffusion before the system reaches to the BEC phase. This approach has been tried in Cu_2O (Refs. 1–3) to find some definite signals indicating the excitonic BEC generation at the center of the trap as actually observed in atomic systems.

Usually, the excitons are loaded in a trap through the dipole-allowed phonon-assisted one-photon absorption process.[1–3] In this case, excess heating due to phonons generated simultaneously with excitons may become an essential factor that prevents the realization of the BEC. We consider that the heating might be minimized by two-photon loading of excitons in the trap.

The above is our motivation of the present work, but the two-photon excitation has an additional advantage that three-dimensional diagnostics of the trap itself is possible in high spatial resolution. This is owing to (1) the spatial change of the two-photon resonance energy of 1*s* yellow excitons reflecting the distribution of the inhomogeneous stress, (2) the sharpness of the resonance, and (3) the increase of the spatial resolution by the nonlinearity in degenerate two-photon excitation regime. In the one-photon excitation scheme, on the other hand, the diagnostics is restricted to one-dimension along the stress and the spatial resolution is lowered, both because of the continuum absorption of the phonon-assisted band.

We have reported luminescence of orthoexcitons in a two-dimensionally (2D) confined 1D shallow exciton trap under two-photon excitation.[4] The results suggest that the temperature of the orthoexciton system is kept low when the excitons are directly created at the center of the trap. In this paper, we present the experimental results on the paraexcitons in a 3D confined exciton trap of deeper depth, in order to examine the feasibility of the two-photon loading scheme for the excitonic BEC.

II. EXPERIMENT

The sample was cut from a naturally grown single crystal of Cu_2O. The surfaces were oriented along (001), (110), and $(1\bar{1}0)$ crystallographic planes. The orientation was confirmed by measured polarization characteristics inherent in the two-photon absorption of the orthoexcitons.[5]

In the present experiment, the primary stress axis was chosen to be parallel to the [110] crystal axis. In this configuration, the green-orthoexciton states of Γ_3^+ and Γ_4^+ symmetry mix to the yellow paraexcitons of Γ_2^+ symmetry. On the other hand, either Γ_3^+ or Γ_4^+ state mixes to the paraexcitons, depending on whether the applied stress is along [100] or [111].[6] The paraexciton lifetime is expected to be shorter in [110] stress than in [100] or [111] stress. Nevertheless, we choose the [110] stress configuration to enhance the luminescence intensity and to improve the S/N ratio in detecting the paraexciton signals.

The sample was immersed in liquid helium at 1.6 K. A glass lens of 3.5 mm curvature was pressed against the top surface of a (110) plane of the sample. The contact between the rounded plunger and the flat crystal surface produces nonuniform strain distribution inside the crystal. Since the energy of the lowest exciton level decreases with increasing shear strain, a trap center where the excitons feel lowest potential energy locates approximately at the point of the maximum shear strain below the contact. In the [110] stress configuration, we observed that two wells of almost identical shape were formed near the top surface.[7] Figure 1 illustrates a cross-sectional view of the well in a $(1\bar{1}0)$ plane: One well locates behind the other when viewing from this face, in which direction direct recombination of paraexcitons is allowed. The solid curves schematically show equipotential contours for the excitons.

A laser beam from a color-center laser (Solar, LF151) was directed to the $(1\bar{1}0)$ face, penetrating the equivalent portions of the two wells. The duration and the repetition rate of the laser light were 12 ns and 400 Hz, respectively. The emission was collected from the other $(1\bar{1}0)$ face and introduced to a high-dispersion monochromator (Jobin Yvon,

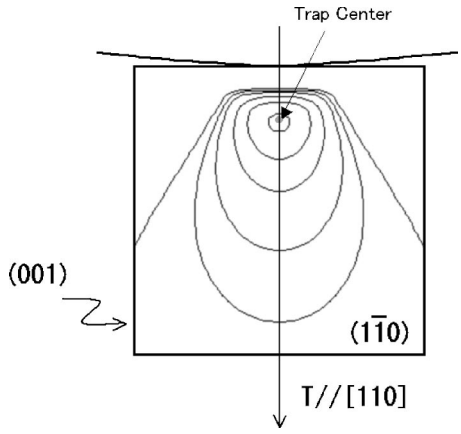

FIG. 1. Schematic view of equipotential curves in a sample having a Hertzian contact to a rounded plunger at the top. The stress maximum, i.e., the trap center, is located inside the crystal below the contact.

THR1500). To obtain the time-resolved emission spectra, a gated ICCD camera system (LaVision, PicoStar HR12) with a 25 cm monochromator (Jasco, CT-250T) was used. The geometry of the excitation and observation was kept the same as the time-integrated measurement.

III. RESULTS AND DISCUSSION

Figure 2 shows time-integrated emission spectra of orthoexcitons and paraexcitons under fixed pressure to the plunger at 1.6 K. The lowest trace shows the emission spectrum when the excitation light was adjusted to the two-photon resonance energy of the 1s orthoexcitons at the trap center. The structures labeled Xo and Xo-Γ_3^- are due to direct and phonon-assisted emission of the orthoexcitons, respectively. A small peak at the high-energy side of Xo-Γ_3^- corresponds to the resonance emission of paraexcitons Xp, which becomes slightly allowed by the mixing effects as mentioned in Sec. II. This observation tells us that paraexcitons are surely generated by downconversion of resonantly produced orthoexcitons.

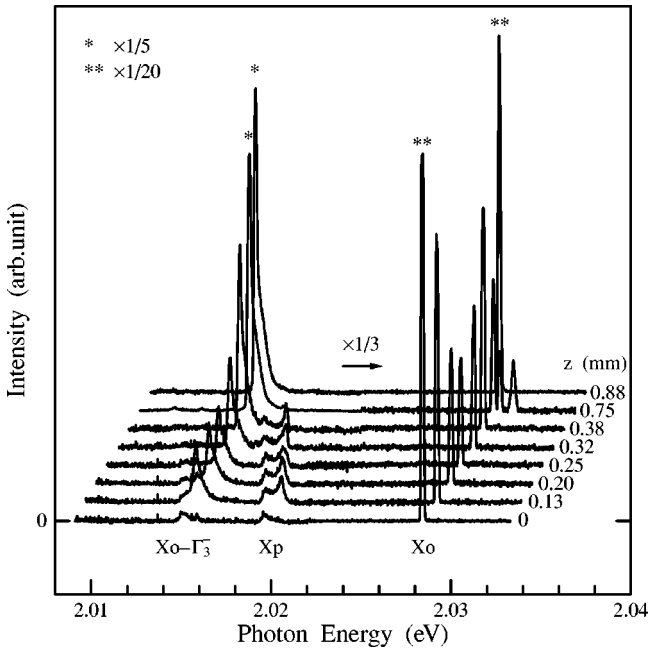

FIG. 2. Time-integrated spectra of phonon-assisted (Xo-Γ_3^-), direct (Xo) emission of orthoexcitons, and direct emission of paraexcitons (Xp). Respective curves were obtained by selective pump at small spots under different magnitudes of the stress.

Emission spectra at less stressed regions were successively obtained in the following procedure: the photon energy of the incident light was increased so as to pump orthoexcitons at the rims of the each trap [i.e., at two points per one well when viewing from (001) face], and then the position of the focusing spot was shifted downward until these two spots merge into one below the trap center. After determining the location z of the excited spots by the vertical position of the luminous spot measured from the trap center, corresponding spectrum was taken. The procedure was repeated until the two-photon energy reached to the orthoexciton resonance under zero stress.

The vertical entrance slit of the monochromator provides spatial integration of the emission in the plane including the primary stress axis and the laser beam path. This means that the monochromator collects the luminescence from the resonantly excited excitons at the pump spot as well as that from drifting ones, provided that the excitons can drift from the initial pump spot to the center of the trap.

As seen in the figure, the intensity of the Xo line depends on the two-photon excitation energy, or the position of the excitation spot.[8] This is presumably caused by the competition between decreasing excitation volume toward the trap center and increasing SHG signal intensity by relaxation of the selection rules for the quadrupole-SHG process.

The potential gradient $F=-dE/dz$ for the orthoexcitons is estimated from the shift of the resonance energy dE and that of the position dz. We certified that F increases toward the trap but turns to decrease in the periphery of the trap center, forming a harmonic potential well for orthoexcitons. The energy shift of the Xo-Γ_3^- band is consistent with the positions of the Xo line. In a similar way, one can estimate the potential gradient for paraexcitons from the positions of the Xp line.

Solid dots in Fig. 3(a) are measured paraexciton energies as a function of the stress. The magnitude of the stress was calibrated by the energy positions of the Xo line shown by open dots. Since the Hertzian contact stress is nearly uniaxial along the primary stress axis except for the region above the trap center (where the hydrostatic stress dominates), we referred to the uniaxial theory[9,10] in the calibration. This theory has successfully explained the results of Raman scattering measurements for orthoexcitons under uniaxial stress along [110] axis.

Solid curves in the figure are calculated orthoexciton energies for the [110] stress configuration (see the Appendix). With 0.4 kbar stress, luminescence from three orthoexciton branches is observed.[6] This is caused by the thermal population between the relevant sub-levels.

The dashed curve is the calculated paraexciton energy as a

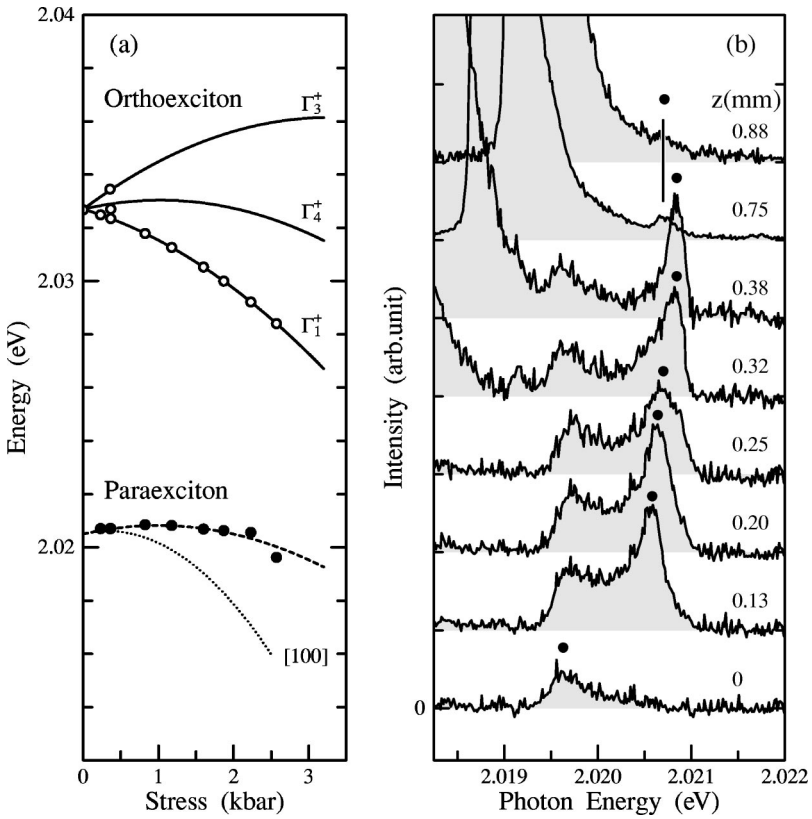

FIG. 3. (a) Paraexciton energy level as a function of the magnitude of the [110] stress, which was deduced from the energy level of the orthoexcitons. Solid curves are calculated orthoexciton energies using Eqs. (A1)–(A3). The dashed line and dotted line correspond to paraexciton levels under [110] and [100] uniaxial stress, respectively. (b) Spectra of the direct emission of paraexcitons (Xp) in an expanded energy scale. The solid dots correspond to the energy level of the paraexcitons at the excitation spot. The low-energy tail is due to drift of paraexcitons into lower potential regions.

function of the stress, which has not been reported as far as we know. It is clear that the measured paraexciton energies (solid dots) are well reproduced by the calculation. The energy shift is smaller compared to the [100] case (dotted curve) but a shallow trap for paraexcitons is still formed in the stress higher than about 2.3 kbar. The depths of the trap in the present conditions are estimated to be 4.3 meV (50 K) and 1.6 meV (19 K) for orthoexcitons and paraexcitons, respectively.

Displayed in Fig. 3(b) are reproductions of the emission spectra of paraexcitons shown in Fig. 2 in an expanded scale. The sharp peaks marked by solid dots are Xp at the excitation spots. At the low-energy side, additional structure appears. The energy position corresponds to the energy of paraexcitons at the trap center. The intensity increases as the pump spot approaches to the trap center (from upper to lower curves).

These features do not contradict with the occurrence of the drift of the paraexcitons. For the drift to take place, the transit time $t=z/F\mu$, should be shorter than the exciton lifetime, where μ is the exciton mobility. As an example, let us consider the case of $z=0.13$ mm. Since the change of the stress during the travel is small, we take the mobility, $\mu \sim 2\times 10^6$ cm^2/eV s,[2] corresponding to the stress of 2.3 kbar at the midpoint of the travel. Using $F\sim 0.03$ eV/cm from the spectroscopic data shown above, one obtains $t\sim 0.2$ μs. This is shorter than the lifetime 0.5 μs of paraexcitons in a trap in high purity crystals reported in the literature.[2] However, the exciton lifetime is known to be strongly dependent on the sample quality, excitation level, and applied stress. Therefore, we must know the paraexciton lifetime in the presently used sample for quantitative discussion.

Figure 4(a) shows examples of time-resolved emission spectrum at 25 ns and 1 μs delay after the laser pulse. The gate width was chosen to be 1 μs. The conditions were almost the same as the above measurement except that applied stress and two-photon energy were slightly decreased to 2.4 kbar and 2.029 eV, respectively. The trap center was directly pumped. The apparent difference between the spectrum at 25 ns delay and the lowest two curves in Fig. 2 is due to the difference in the spectral resolution. In the time-resolved spectrum, the phonon-assisted band of paraexcitons (X_p-Γ_5^-) is slightly seen owing to the improvement of the *S/N*.

Plotted in Fig. 4(b) is the integrated intensity of the Xp line as a function of time. It was found that Xp shows much slower decay than luminescence associated with orthoexcitons. The initial decay with $\tau_{\rm trap}=0.3$ μs and subsequent slower decay were observed.

Similar double exponential decay was also reported for high-density excitation in the one-photon regime.[1] The reason has not been given, but the orthoexciton decay is known to slow down by Auger process in which two paraexcitons collide to form an orthoexciton. In the present experiment, orthoexcitons show a fast decay indicating that paraexciton density is not so high as the Auger process becomes significant. The reason why the paraexcitons exhibit a double exponential decay is not clear at the moment. Nevertheless, the estimated transit time is shorter even than the faster decay time $\tau_{\rm trap}$.

As another example, let us consider the case of $z=0.25$ mm. The exciton lifetime is expected to be longer

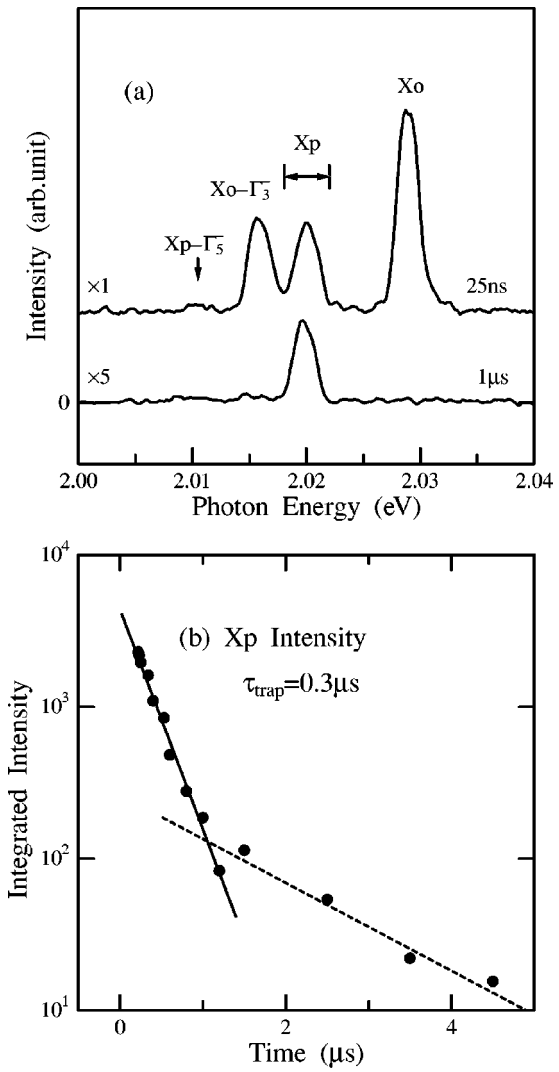

FIG. 4. (a) Time-resolved luminescence spectra under resonance excitation at the center of the trap, produced by 2.4 kbar stress. (b) Intensity of the paraexciton emission Xp as a function of time. The range of the spectral integration is indicated by the horizontal arrow in (a).

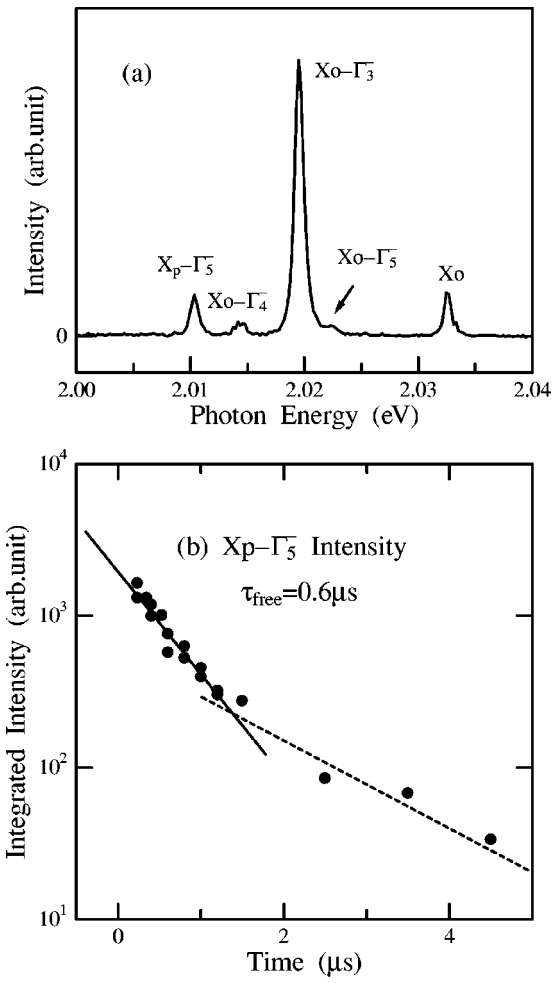

FIG. 5. (a) Time-resolved luminescence spectrum under zero stress at 25 ns delay with 1 μs gate width. Xo-Γ_4^- and Xo-Γ_5^- are phonon-assisted bands of orthoexcitons involving phonons of Γ_4^- and Γ_5^- symmetry, respectively. (b) Decay of the phonon-assisted band of paraexcitons (Xp-Γ_5^-) under zero stress.

in less stressed regions. Therefore, the upper bound of the lifetime of excitons in a trap should be given by the decay time under zero stress.

Figure 5(a) shows the spectrum of Xp-Γ_5^- band with zero stress applied to the sample. Note that the direct recombination of paraexcitons (Xp) is forbidden under zero stress, as confirmed by the spectrum. Figure 5(b) shows emission intensity of Xp-Γ_5^- band as a function of time. The decay was again composed of two parts with the initial decay time of $\tau_{\text{free}}=0.6$ μs. Accordingly, it is reasonable to assume that the paraexciton decay ranges from $\tau_{\text{trap}}(=0.3$ μs) to τ_{free} depending on the locations in the trap.

During the travel over about twice the distance as the former case, F and μ also change. Namely, F has the maximum value near $z=0.1$ mm while μ is lower at more highly stressed regions. Nevertheless, the drift speed is given by the product of F and μ, and does not largely differ during the travel. Using $z=0.25$ mm and relevant approximated values at the midpoint ($F=0.02$ eV/cm and $\mu=3\times10^6$ cm^2/eV s), the transit time is 0.4 μs, comparable to the lifetime.

The above considerations lead us to conclude that paraexcitons can drift from the rim to the center of the trap. The slight increase of the drift component from upper to lower trace in Fig. 3(b) suggests that the number of cold paraexcitons increases as the pump spot moves in. This means that the two-photon loading scheme is useful for creating such cold paraexcitons near the trap center. Recently, Schmitt *et al.* theoretically discussed the trapping kinetics toward the BEC of excitons in a shallow potential well in Cu_2O.[11] Their approach should be applicable to our deeper well.

In our experiments, the maximum density of the excitation is limited to avoid the radiation damage on the crystal surfaces. If more effective means to increase the number of excitons at low temperature was developed, the BEC might be realized along the present scenario.

IV. CONCLUSION

We performed luminescence spectroscopy on 1s yellow excitons in a strain-induced trap in Cu_2O at 1.6 K in two-photon excitation regime. It was proved that paraexcitons are generated via cold orthoexcitons pumped by the two-photon resonance. The Hertzian contact stress along [110] axis was found to create potential traps for orthoexcitons and paraexcitons. The direct and phonon-assisted emission of the paraexcitons was observed under the resonant two-photon excitation of 1*s* orthoexcitons. The drift of the paraexcitons was studied in the spectral domain. The transit time is consistent with the measured decay time of the emission of the paraexcitons.

ACKNOWLEDGMENTS

We would like to thank T. Ueda and T. Nishi (Marubun corporation) who kindly gave us an opportunity to use the ICCD-camera system. One of the authors (N. Naka) thanks D. W. Snoke (Univ. Pittsburgh) for helpful conversations on the levelshift of paraexcitons. This work was partially supported by The Mitsubishi Foundation for Scientific Researches and the grant-in-aid for scientific research from The Ministry of Education, Science and Culture, Japan.

APPENDIX: EXCITON ENERGY SHIFT UNDER [110] STRESS

Orthoexciton levels under [100] and [110] uniaxial stress have been experimentally obtained by Raman scattering measurement.[9] The energy shift as a function of the magnitude of the [100] stress was explained by using Pikus-Bir strain Hamiltonian for stress-dependent valence band splitting. Analyzing the [100] data with an assumption that the spin-orbit splitting Δ' is 74 meV,[12] Waters *et al.* obtained exchange energy J and deformation potentials a,b. Information on the shear deformation potential, d, is not obtained from the analysis of [100] data. Trebin *et al.* later proposed a theory which covers [100], [111], and [110] cases.[10] Using matrices (14) and Table III of Ref. 10, we obtained the explicit forms for energy shifts of three orthoexciton branches under uniaxial [110] stress of magnitude T:

TABLE I. Parameters used in the stress calculation.

parameters	values	values	
h	-0.64	-0.50	meV/kbar
e	7.9	5.8	meV/kbar
f	-2.6		meV/kbar
Δ'	128	74	meV
J	-18.0	-22.7	meV

[a]From Ref. 10.
[b]From Ref. 9

$$E^{110}_{\Gamma_3^+}=hT+\frac{2J}{3\Delta'}(e-3f)T-\frac{1}{2\Delta'}(e^2+3f^2)T^2, \quad \text{(A1)}$$

$$E^{110}_{\Gamma_4^+}=hT+\frac{2J}{3\Delta'}(e+3f)T-\frac{1}{2\Delta'}(e^2+3f^2)T^2, \quad \text{(A2)}$$

$$E^{110}_{\Gamma_1^+}=hT-\frac{4Je}{3\Delta'}T-\frac{1}{2\Delta'}(e^2+3f^2)T^2, \quad \text{(A3)}$$

and the paraexciton energy

$$E^{110}_{\text{para}}=hT-\frac{1}{2\Delta'}(e^2+3f^2)T^2, \quad \text{(A4)}$$

where $h=a(s_{11}+2s_{12}), e=3b(s_{11}-s_{12})$, and $f=-(\sqrt{3}d/2)s_{44}$ with cubic elastic compliance constants, s_{11}, s_{12}, and s_{44}. $\Gamma_i^+(i=1,3,4)$ in the subscript of orthoexciton energy denotes the symmetry of the relevant state.

Since paraexciton levelshift under [110] stress has not been taken up so far, we calculated paraexciton energy using Eq. (A4) with parameters determined by Trebin *et al.* The values used in the calculation are listed in the second column of Table I, in comparison with those by Waters *et al.* in the third column.

[1] D.P. Trauernicht, J.P. Wolfe, and A. Mysyrowicz, Phys. Rev. B **34**, 2561 (1986).
[2] D.P. Trauernicht and J.P. Wolfe, Phys. Rev. B **33**, 8506 (1986).
[3] D.W. Snoke and V. Negoita, Phys. Rev. B **61**, 2904 (2000).
[4] N. Naka and N. Nagasawa, J. Lumin. **87-89**, 201 (2000).
[5] S. Kono, M. Hasuo, and N. Nagasawa, J. Lumin. **66/67**, 433 (1996).
[6] F.I. Kreingol'd and V.L. Makarov, Sov. Phys. Semicond. **8**, 962 (1975).
[7] We thank J.P. Wolfe and J. Jang (Univ. Illinois) for the discussion on the double-well formation.
[8] In high-resolution spectroscopy, the intensity of the *Xo* line diminishes at just the resonance [N. Naka and N. Nagasawa, Solid State Commun. **110**, 153 (1999)]. This effect can be neglected in the present experiment because the laser linewidth was not narrow enough for such observations.
[9] R.G. Waters, F.H. Pollak, R.H. Bruce, and H.Z. Cummins, Phys. Rev. B **21**, 1665 (1980).
[10] H.-R. Trebin, H.Z. Cummins, and J.L. Birman, Phys. Rev. B **23**, 597 (1981).
[11] A. Schmitt, L. Bányai, and H. Haug, Phys. Rev. B **63**, 205113 (2001).
[12] The spin-orbit splitting $\Delta'=74$ meV in Ref. 9 was deduced from the hydrogenic energy relation for *p*-series excitons assuming small central cell correction. Actually, this assumption is not true for 1*s* excitons of our present interest. The correction is taken into account in Ref. 10.